Hindawi
Advances in Materials Science and Engineering
Volume 2018, Article ID 7814039, 12 pages
https://doi.org/10.1155/2018/7814039

Research Article

Investigation of Performance and Residual Stress Generation of AlSi10Mg Processed by Selective Laser Melting

Lianfeng Wang,[1,2,3] Xiaohui Jiang,[4] Yihong Zhu,[4] Zishan Ding,[4] Xiaogang Zhu,[2] Jing Sun,[2] and Biao Yan[1]

[1]*School of Materials Science and Engineering, Tongji University, Shanghai 201804, China*
[2]*Shanghai Aerospace equipment Manufacturer Co.,Ltd, Shanghai 200245, China*
[3]*Shanghai Research Center of Complex Metal Parts by Additive Manufacturing, Shanghai 200245, China*
[4]*College of Mechanical Engineering, University of Shanghai for Science and Technology, Shanghai 200093, China*

Correspondence should be addressed to Xiaohui Jiang; jiangxh@usst.edu.cn and Biao Yan; tjyanbiao@163.com

Received 14 November 2017; Revised 4 February 2018; Accepted 20 February 2018; Published 3 April 2018

Academic Editor: Michael J. Schütze

During the selective laser melting (SLM) process, the scanned layers are subjected to rapid thermal cycles. By working on the mechanical properties, residual stress, and microstructure, the high-temperature gradients can have significant effect on the proper functioning and the structural integrity of built parts. This work presents a comprehensive study on the scanning path type and preheating temperature for AlSi10Mg alloy during SLM. According to the results, SLM AlSi10Mg parts fabricated in chessboard scanning strategy have higher mechanical properties or at least comparable to the parts fabricated in uniformity scanning strategy. In the SLM processing, the residual stress in different parts of the specimen varies with temperature gradient, and the residual stress at the edge of the specimen is obviously larger than that at the center. Under the chessboard scanning and preheating temperature 160°C, the residual stress in each direction of the specimens reaches the minimum. Under different forming processes, the morphology of the microstructure is obviously different. With the increase of preheating temperature, the molten pool in the side surface is obviously elongated and highly unevenly distributed. From the coupling relationship between the residual stress and microstructure, it can be found that the microstructure of top surface is affected by residual stresses σx and σy. But the side surface is mainly governed by residual stress σy; moreover, the greater the residual stress, the more obvious the grain tilt. In the XY and XZ surfaces, the scanning strategy has little influence on the tilt angle of the grain. But, the tilt angle and morphology of the microstructure are obviously affected by the preheating temperature. The results show that the residual stresses can effectively change the properties of the materials under the combined influence of scanning strategy and preheating temperature.

1. Introduction

Selective laser melting (SLM) is one of the most common ways of additive manufacturing and usually used to produce components with desired complex internal structures, and it yields shortened product development cycles [1]. Particle reinforced aluminum matrix composites (AMCs), because of its low density, high strength, low coefficient of thermal expansion, and outstanding abrasion resistance, can meet these requirements well accordingly, which have been widely used in the industrial fields of aerospace, automotives, and microelectronics [2–4]. AlSi10Mg is an important alloy to be processed by the SLM process due to small differences in its melting and solidification temperatures [5]. Prashanth et al. [6] studied the properties of five different metals/alloys (Al–12Si, Cu–10Sn, and 316L (face centered cubic structure) and CoCrMo and commercially pure Ti (CP–Ti) (hexagonal close packed structure)), fabricated by selective laser melting, found that selective laser melting is a reliable fabrication method to produce metallic materials with consistent and reproducible properties. In SLM, a complex heat effect acts on the material, resulting in a different heat transfer mechanism compared with that in casting and forging. During the construction process, however,

thermally induced residual stress occurs due to the layered build-up and the local input of energy by means of a focused laser beam, which can lead to distortion of the component or sections of the component itself [7]. Rapid cooling results in a nonequilibrium solidification process and enhances the limitation of solid solubility, refinement of grains, and possible formation of new metastable phases, even amorphous phases [8]. However, large temperature gradients and complex heat transfer form in a molten pool, which can cause preferential grain growth and heterogeneous structure [9]. Buchbinder et al. [7] found that when the substrate plate heated during the construction process, the effects could be reduced or eliminated entirely. Prashanth et al. [10] found that the equation currently used to calculate the energy density gives only an approximate estimation, in either case with a decrease in the laser power the tensile properties deteriorate because of the increasing amount of keyhole porosity and suggests that the laser power is one of the most influencing process parameters to be considered. At the same time, Kempen et al. [11] investigated the effect of processing parameters on the shape of single track and molten pool based on the AlSi10Mg alloy and pronounced that the good surface quality of single track can produce using optimal processing parameters (namely, scan speed, laser power, and scan spacing). Buchbinder et al. [12] have demonstrated that the processing parameters have a significant influence on the density of as-build AlSi10Mg alloy parts due to the existence of pores. Prashanth et al. [13] evaluated the influence of different processing parameters on the room temperature tensile properties; they found that the room temperature tensile properties can be tuned in-situ during the selective laser melting process giving an opportunity to define the mechanical properties of the SLM parts to suit their service requirements. Salari-Sharif et al. [14] used a variety of measuring techniques (SEM imaging, CT scanning, and so on) to characterize the geometric imperfections in a nickel-based ultralight hollow microlattice and investigated their effects on the compressive strength of the lattice. Unfortunately, because of the high cooling rate and thermal inhomogeneity in the process of the SLM, there is a large temperature gradient between the sample and the substrate. It will have a very important influence on the solidification microstructure of metal forming parts and then directly affects the macroproperties such as the crack and deformation. So how to change the temperature distribution, reduce the temperature gradient and thermal stress in the process of forming, and to prevent crack caused in the process of SLM has become an urgent problem, which needs to be solved. Nonetheless, a systematic investigation of the extent to effects of preheating and scanning strategy on residual stress and microstructure of aluminum components has not yet fully analyzed. This works aims to systematically investigate the effects of thermal behavior during SLM of aluminum components, to explore the relationship between the residual stress and the microstructure of SLM by effectively controlling the thermal effect of the material, to achieve further optimization, and to improve the quality of the specimen during SLM.

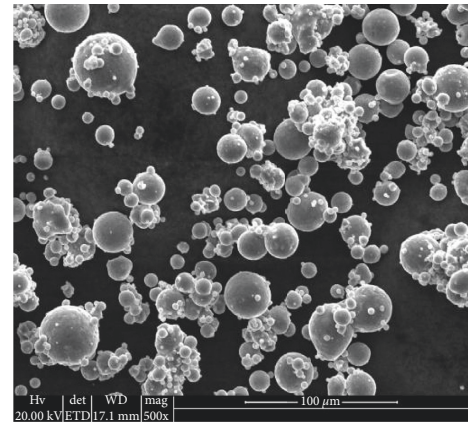

Figure 1: SEM image of the AlSi10Mg alloy.

Table 1: Chemical composition of the AlSi10Mg alloy (wt.%).

Al	Si	Mg	Fe	Cu	Mn	Others
Balance	9.0~10.0	0.40~0.60	≤2.0	≤0.60	≤0.35	≤0.25

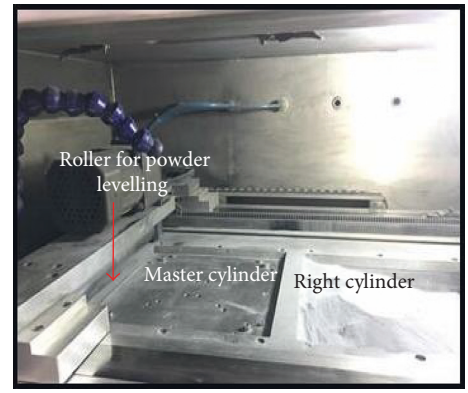

Figure 2: The SLM manufacturing system.

2. Materials and Methods

2.1. Materials. The experimental powder of the AlSi10Mg alloy was shown in Figure 1. The powder morphology is spherical, and the particle diameter is in the range of 20~63 μm. The powder contains a large amount of small particles, which may negatively affect their flow ability due to the small particles agglomerate. However, the small particles may significantly increase the specific surface area of material, leading to high energy absorptivity of the laser beam [15]. The chemical composition of the AlSi10Mg alloy powder is presented in Table 1.

2.2. Methods. The experimental device using $250 \times 250 \times 250\ \text{mm}^3$ building room equipment constitutes "Space M200 type" SLM manufacturing systems, as shown in Figure 2. In order to study the effect of the scanning strategy and the substrate preheating on the samples. The processing parameters are as shown in Table 2.

Table 2: SLM processing conditions.

Processing parameters	Value
Laser power, P	400 W
Scanning speed, v	500 mm/s
Powder layer thickness, h	30 μm
Scan spacing, d	150 μm
The substrate preheating temperature	80°C, 120°C, and 160°C
Scan strategy	Uniformity scanning and chessboard scanning

Table 3: Mechanical properties of SLM AlSi10Mg samples.

	Sample number	Tensile strength (R_m/MPa)	Elongation (δ5%)	Impact energy	Hardness (Hv10)	Density	
						Absolute value (g/cm^3)	Relative value (%)
Uniformity scanning, preheat to 80°C	1	327.0	2	4.8	172	2.62	97.76
	2	295.0	2.5	4.7	173	2.62	97.76
	3	288.0	1.5	4.9	165	2.62	97.76
	Average	303.3	2	4.8	170	2.62	97.76
Chessboard scanning, preheat to 80°C	1	391.0	4	6.1	176	2.66	98.88
	2	381.0	3.5	6.3	170	2.64	98.50
	3	383.0	1.5	6.1	182	2.65	98.69
	Average	385.0	3	6.17	176	2.65	98.69
Uniformity scanning, preheat to 120°C	1	308.3	1.69	4.3	247	2.604	97.16
	2	306.1	1.80	4.1	253	2.608	97.31
	3	316.2	2	4.2	247	2.606	97.24
	Average	310.2	1.83	4.2	249	2.606	97.24
Chessboard scanning, preheat to 120°C	1	383.0	2.5	5.4	252	2.60	97.01
	2	383.0	3	5.2	253	2.61	97.39
	3	378.0	3	5.4	266	2.62	97.76
	Average	381.3	2.83	5.33	257	2.61	97.39
Uniformity scanning, preheat to 160°C	1	310.0	5.4	1.7	231	2.59	97.00
	2	300.3	3.6	1.5	220	2.58	97.00
	3	299.0	3.6	1.7	227	2.58	97.00
	Average	303.1	4.2	1.63	226	2.583	97.00
Chessboard scanning, preheat to 160°C	1	370.0	6	2.2	229	2.60	97.01
	2	375.0	5	1.9	233	2.60	97.01
	3	346.0	5	2.2	236	2.60	97.01
	Average	363.7	5.33	2.1	233	2.60	97.01

Before the experiment, in order to remove the water contained in the powder, the powder is kept in the drying oven for heating and drying process. In addition, the heating temperature is 80°C and the holding time is 4 h so that it can improve the flow ability of powders. On the other hand, it can also prevent the formation of pores in the powder-dissolved water to produce hydrogen in the SLM. Note that, before laser scanning, the building chamber was sealed and the purity argon gas was fed inside, thereby decreasing the oxygen content below 0.01 vol.% because oxygen can react with Al or Mg leading to embrittlement of samples [16].

The microstructure was characterized by optical microscopy using the Axio Observer 3 m microscope, and density analysis was performed by Quartz AU-120PM. Mechanical tests (including tensile strength, elongation, impact energy, and hardness) were carried out using INSTRON Legend MDX.

3. Results and Discussion

3.1. Characterization of Samples. Mechanical properties obtained from the tests made on samples fabricated in chessboard and uniformity scanning path under different preheating temperatures are shown in Table 3. The given values represent the mean values for three specimens. The theoretical density of the AlSi10Mg alloy forging parts is 2.68 g/cm^3, the AlSi10Mg samples prepared by SLM (without subsequent heat treatment) have good compactness, the density can reach more than 97%, and the highest value is 98.88%. With the increasing substrate's preheating temperature, the density of the sample decreased slightly. This is because the melting point of aluminum alloy is relatively low; with the increase of preheating temperature, the metal fluidity is increased, the residence time of the liquid is prolonged, and the perturbation of the metal solution is increased.

The tensile properties and plasticity of the AlSi10Mg specimens prepared at different preheating temperatures in SLM are higher than homogeneous casting parts. Under the preheating temperature 80°C and chessboard scanning, the tensile strength of the specimen is 385 MPa, much higher than the casting (280~310 MPa) and close to the forgings (400 MPa or so), and the elongation is higher than the casting level (casting elongation 2%~3%).

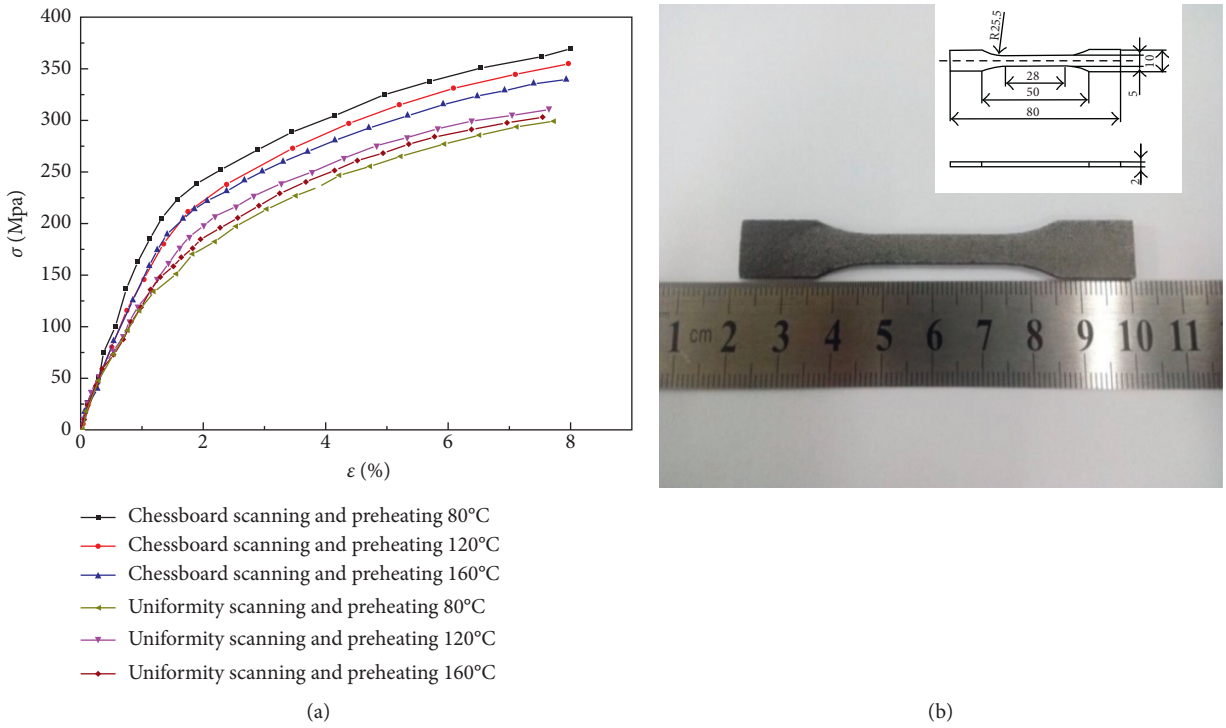

Figure 3: (a) The plots of engineering stress-strain curves of test samples manufactured at different preheating temperatures and scanning modes. (b) Dimensions and actual photographs of tensile specimens.

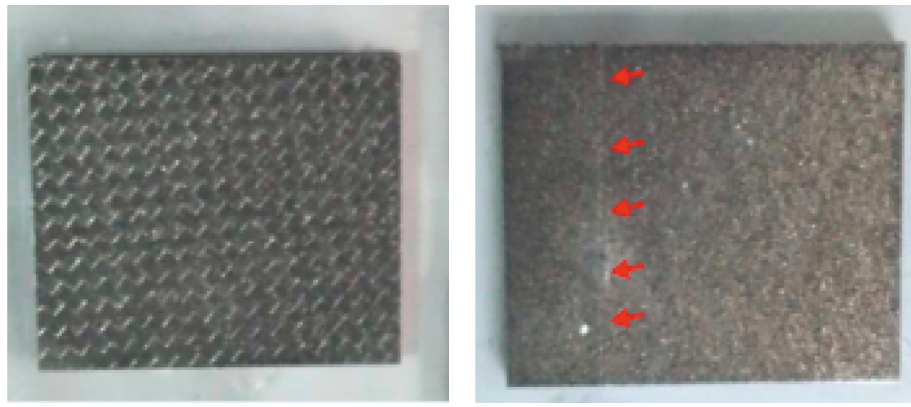

Figure 4: The surface quality of the specimen. (a) Chessboard scanning. (b) Uniformity scanning.

Under the chessboard type scanning and preheating temperature 120°C, the tensile strength and breaking elongation decreased slightly compared to 80°C, but the difference is small. In 160°C, the tensile strength is about 363 MPa, and the elongation is 5.33%.

The impact energy of materials is an important index to measure the toughness of materials. It is sensitive to the internal defects and microstructure of specimens, such as inclusions, segregation, cracks, bubbles, and so on. Under the chessboard scanning and preheating temperature 80°C, the impact energy was up to 6.17 J, and with the increasing of the preheating temperature, the impact energy decreased. In the 160°C, the impact energy decreased sharply as 2.1 J. Through the data comparison, it can found that the preheating temperature has a certain impact on the impact energy, but the role of scanning strategy is more important.

The hardness is affected by the heat treatment and lattice distortion; the experimental results show that, in the SLM process, the preheating temperature has a greater impact on the hardness. Under the preheating temperature 120°C and chessboard scanning, the sample has the largest hardness.

It is observed from Figure 3(a) that the tensile strength of the specimens varies from 303.1 MPa to 385 MPa. The ductility of the samples is divided into 7%~8% which shows the consistency with tensile properties. Under the same chessboard scanning strategy, the maximum difference of ultimate tensile strength of the specimens under preheating temperatures of 80°C, 120°C, and 160°C is about 5.5%

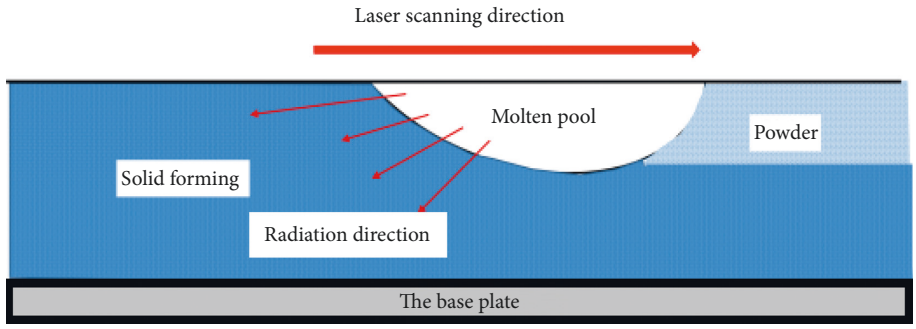

Figure 5: Scatter heat diagram in the SLM process.

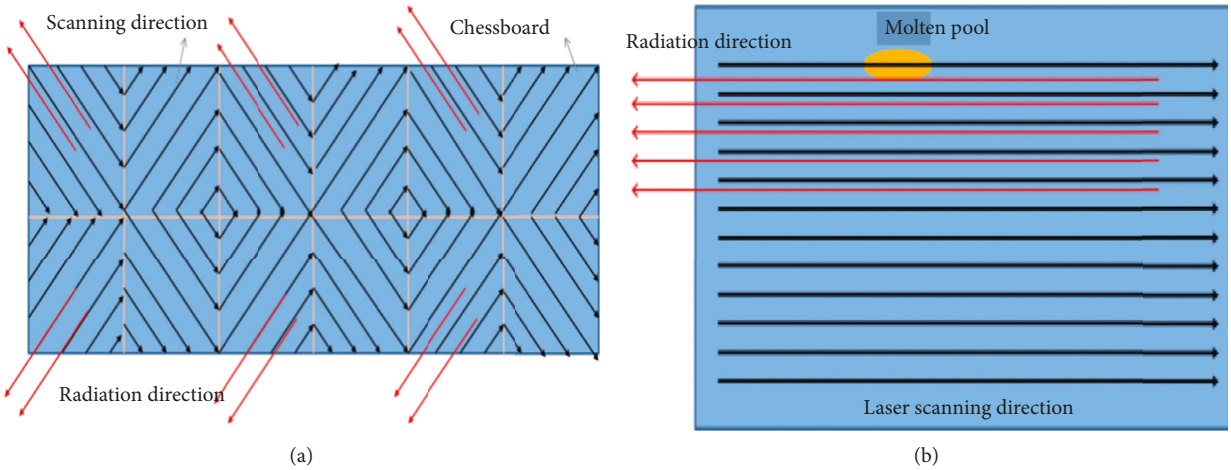

Figure 6: Radiation diagram under different scanning strategies. (a) Chessboard scanning. (b) Uniformity scanning.

(i.e., the difference between the specimens under process parameters of the preheating temperatures 80°C and 160°C). Similarly, under the uniform scanning strategy, the maximum difference of tensile strength between specimens is 2.2% for the preheating temperatures 120°C and 160°C. It is shown from the diagram that, under the same uniform scanning strategy, the tensile effect is obviously worse than the chessboard scanning strategy. Under the condition of controlling a single variable, the scanning method is more effective than the preheating temperature in improving the tensile properties of the specimens. Therefore, the chessboard scanning strategy can be preferred in the manufacture of high tensile properties.

3.2. The Influence of Preheating Temperature and Scanning Mode on SLM Specimen Quality. The surface quality of samples under different scanning strategies is shown in Figure 4 However, compared with the machining process and precision forging, the surface quality of the parts fabricated in SLM shows higher surface roughness and surface oxidation. The surface roughness Ra yields 10–15 μm [17]. Figure 4(a) is under the condition of the preheating temperature of 80°C and the chessboard scanning; the sample surface is smooth, and there is no obvious buckling deformation. Figure 4(b) is under the condition of the preheating temperature 80°C and uniformity scanning. The rough surface can be observed; it is because the accumulative

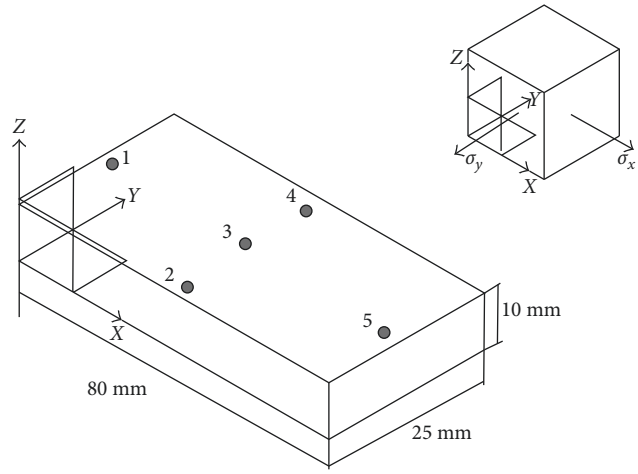

Figure 7: Distribution of test points and stress direction of single point.

deformation and the specimen surface appear protruding prismoid, where the red arrow marks areas.

The scanning strategy in SLM mainly affects the heat dissipation and then affects the microstructure of samples. The scatter heat diagram in the SLM process is presented in Figure 5, in parallel to the laser scanning direction; the molten pool is elongated, and the heat radiation direction is

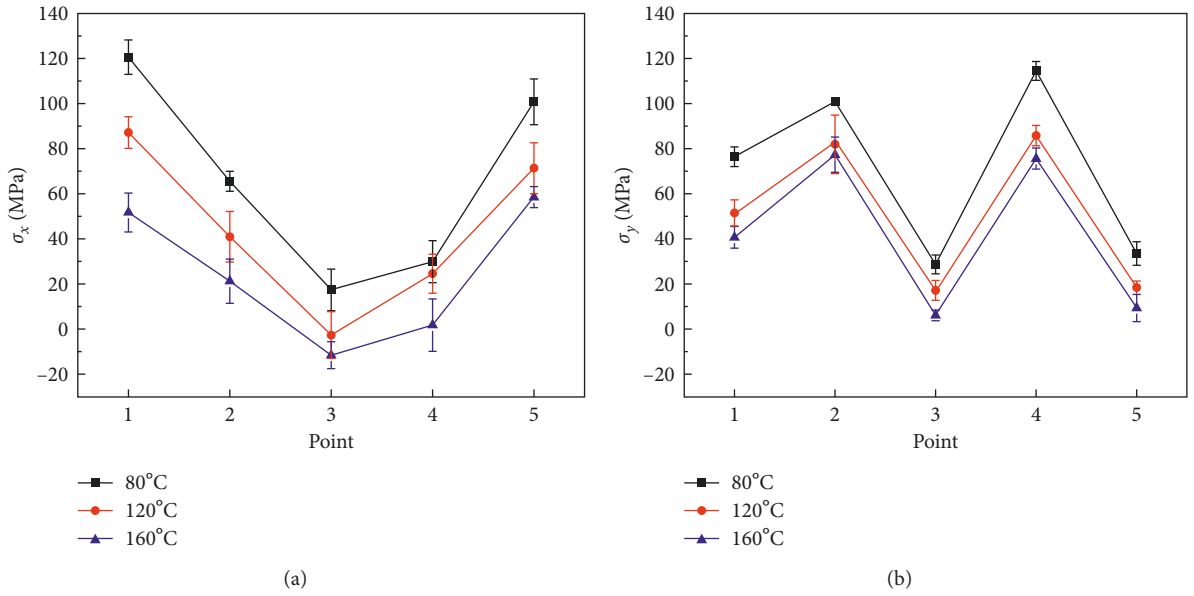

Figure 8: Chessboard scanning. (a) Residual stress in X direction. (b) Residual stress in Y direction.

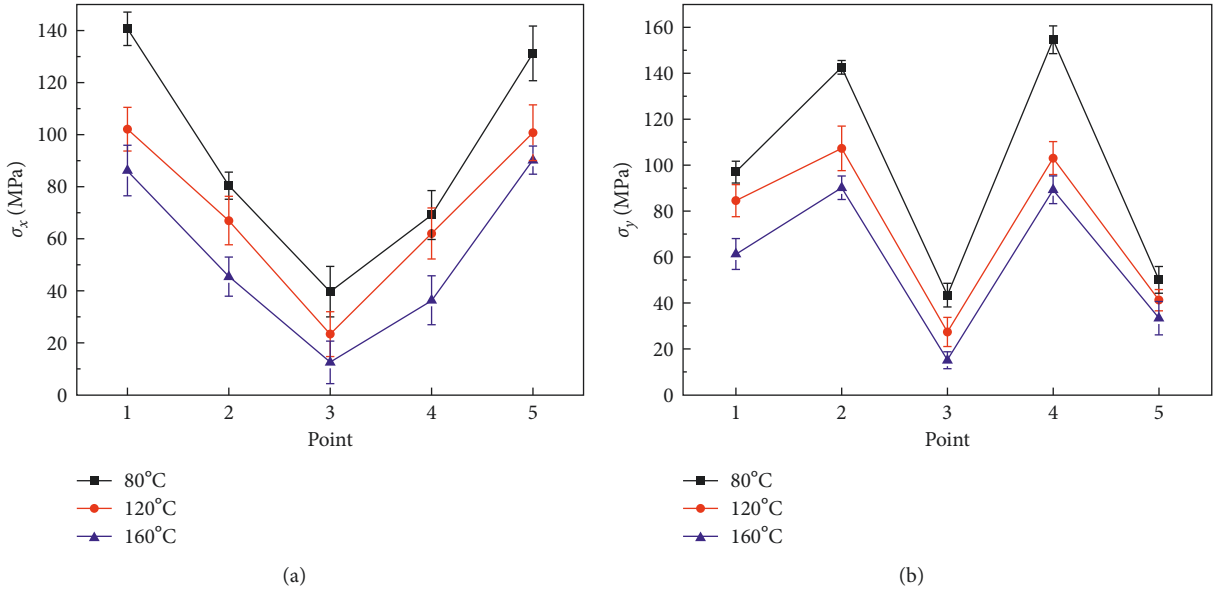

Figure 9: Uniformity scanning. (a) Residual stress in X direction. (b) Residual stress in Y direction.

generally opposite to the laser motion direction. In using chessboard scanning, each chessboard is a scatter heat unit, and the cooling direction is diversified, as shown in Figure 6(a); the scatter heat does not produce large temperature gradient, and the heat will not be accumulated. With chessboard scanning strategy, the heat dissipation is faster, and the sample has less defects and less internal stress. In the uniform scanning strategy, as shown in Figure 6(b), the entire cross section of the specimen is a heat dissipation unit, and the heat dissipation direction is single; it is easy to produce more defects and internal stress accumulation, but it is suitable for the manufacturing of thin-walled part. The experimental results were similar to the study of Xi and Gao [18], who studied the effect of the scanning method on the properties of the laser rapid prototyping TA15 titanium alloy. The results show that the scanning method can significantly refine the microstructure of titanium alloy. Compared with the samples prepared by the uniform scanning strategy, the preparation of the sample under the chessboard scanning strategy can have higher mechanical properties.

3.3. Microstructure and Residual Stress of Samples

3.3.1. The Residual Stress Distribution under Different Processing Methods. The specimens with different preheating temperatures and scanning strategies were used to measure the residual stresses σ_x and σ_y on the XY (top surface) by X-ray diffraction method. The distribution of test points is shown

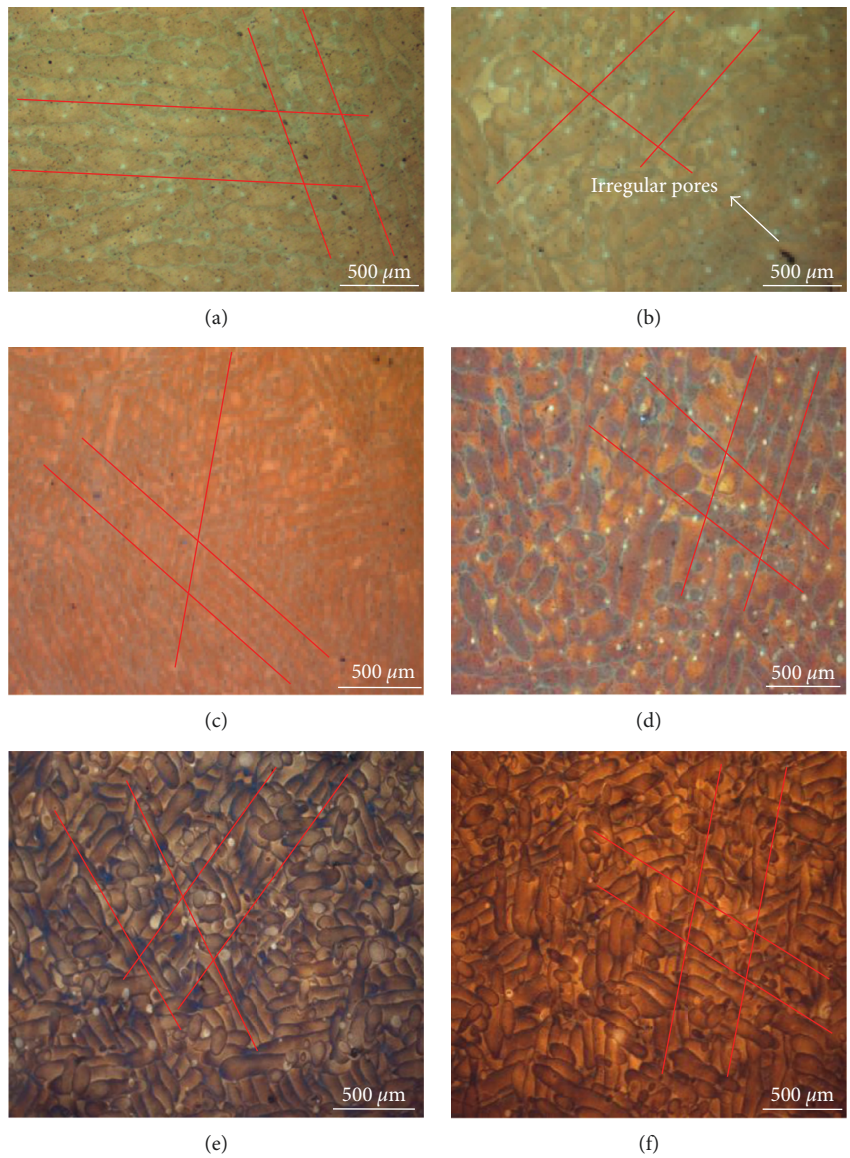

Figure 10: The typical etched morphology of vertical section surface of SLM-processed AlSi10Mg samples at (a) chessboard scanning, preheating temperature of 80°C; (b) chessboard scanning, preheating temperature of 120°C; (c) chessboard scanning, preheating temperature of 160°C; (d) uniformity scanning, preheating temperature of 80°C; (e) uniformity scanning, preheating temperature of 120°C; and (f) uniformity scanning, preheating temperature of 160°C.

in Figure 7, and the residual stress is shown in Figures 8 and 9. Macroscopic stress in the SLM process is caused by two main mechanisms. First, given the Gaussian distribution of laser energy along the horizontal direction, high temperature gradient (thousands of degrees Celsius per mm) can occur in the laser effect area, while nonuniform deformation formed in the following cooling procedure, thereby causing residual stress [19]. Second, the heat transfer between two layers is poor along the height direction, leading to temperature gradient, forming tensile stress in the upper section, and compressive stress in the bottom section [20]. According to the comparison of residual stress data, it is observed that the residual stresses of the specimens under the chessboard scanning strategy are much smaller than that of the uniformity scanning method. Based on the stress field of simulation results, Gusarov et al. [21] reported that residual stress can be reduced by improving the SLM preheating temperature. In this test, regardless of the type uniformity scanning strategy or the chessboard scanning, as the preheating temperature rises from 80°C, 120°C, to 160°C, the residual stress values at each test point are significantly lower. As the substrate preheating temperature rises from 80°C to 160°C, Figure 8(a), point 1, the residual stress value is down by 57%. Compared with the uniformity scanning strategy, the chessboard scanning strategy has shorter scanning path, the processing time interval of the two adjacent scanning lines becomes smaller, and the energy dissipation is reduced. So the energy accumulation is increased. The molten pool has high temperature during the processing; under the effect of preheating, the molten pool accessories substrate temperature is also high, so it is more advantageous to reduce the temperature difference

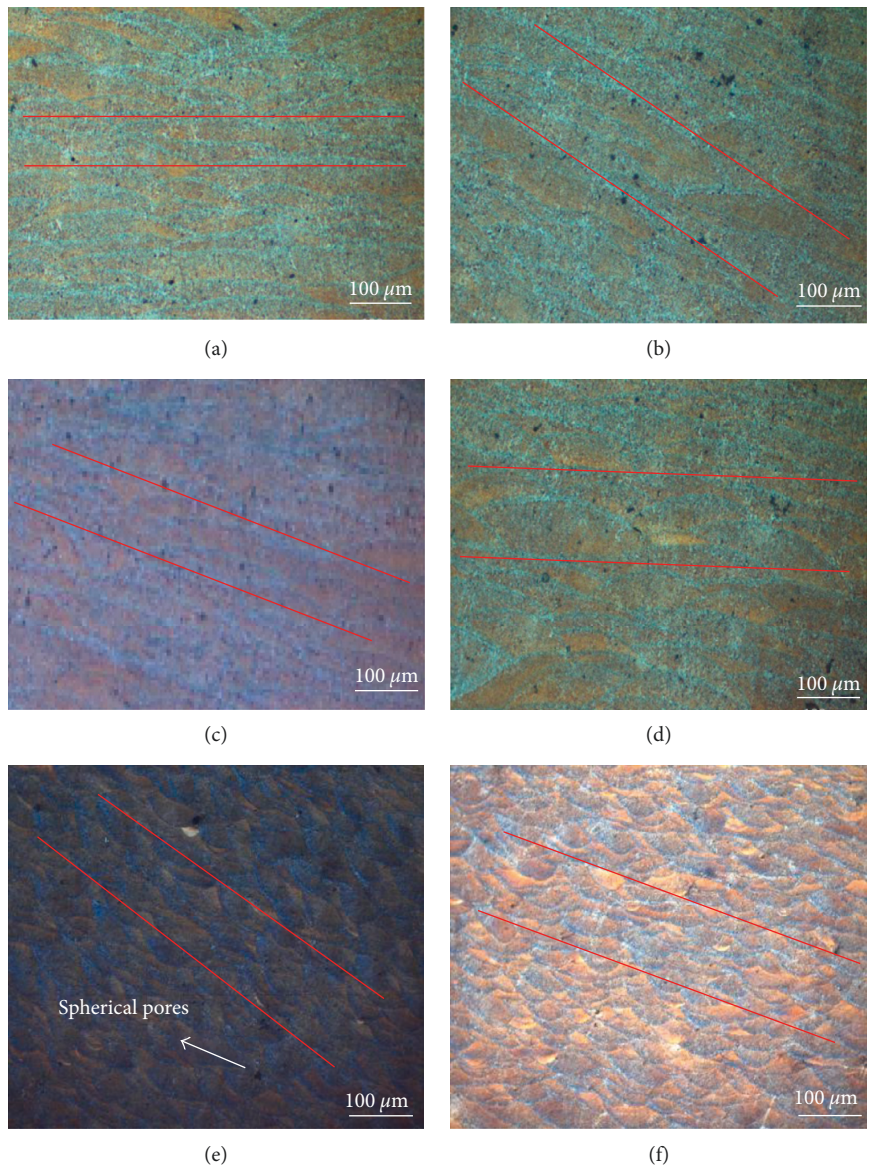

Figure 11: The typical etched morphology of cross section surface of SLM-processed AlSi10Mg samples at (a) chessboard scanning, preheating temperature of 80°C; (b) chessboard scanning, preheating temperature of 120°C; (c) chessboard scanning, preheating temperature of 160°C; (d) uniformity scanning, preheating temperature of 80°C; (e) uniformity scanning, preheating temperature of 120°C; and (f) uniformity scanning, preheating temperature of 160°C.

around the pool and extend the molten pool solidification time. At the same time, it is also beneficial to the overflow of gas inside the pool and the growth of the columnar crystal. Therefore, it can reduce the residual stress of the specimen.

From Figures 8 and 9, it can be noted that, in the X direction (Figures 8(a) and 9(a)), the residual stresses of the test points are distributed in "V" trends; the residual stresses of points 1 and 5 are greater than that of the points 2 and 4. In the X direction, despite the use of chessboard scanning strategy and the preheating, the temperature gradient generated by a longer distance will still lead to the existence of large residual stress at both ends.

In the Y direction (Figures 8(b) and 9(b)), the residual stress of the test points are distributed in "M" trends. However, contrary to the discussion above, the residual stresses of points 1 and 5 are less than that of the points 2 and 4. The reason for this difference is subjected to the combined force of the solid on both sides of the X direction. In the X direction, compared to point 1 and point 3, one side is adjacent to the edge of the specimen. The marginal force acting on the test point is ignored. Points 1 and 3 are governed only by the force acting on one side of the X, and therefore, it will produce this effect. Similarly, this interpretation applies to the phenomenon in Figures 8(b) and 9(b). Hence, through reasonable design of the structure of the specimens, it can effectively avoid the uneven distribution of residual stress.

3.3.2. The Microstructure under Different Preheating Temperatures and Scanning Types. Figures 10 and 11 are the OM

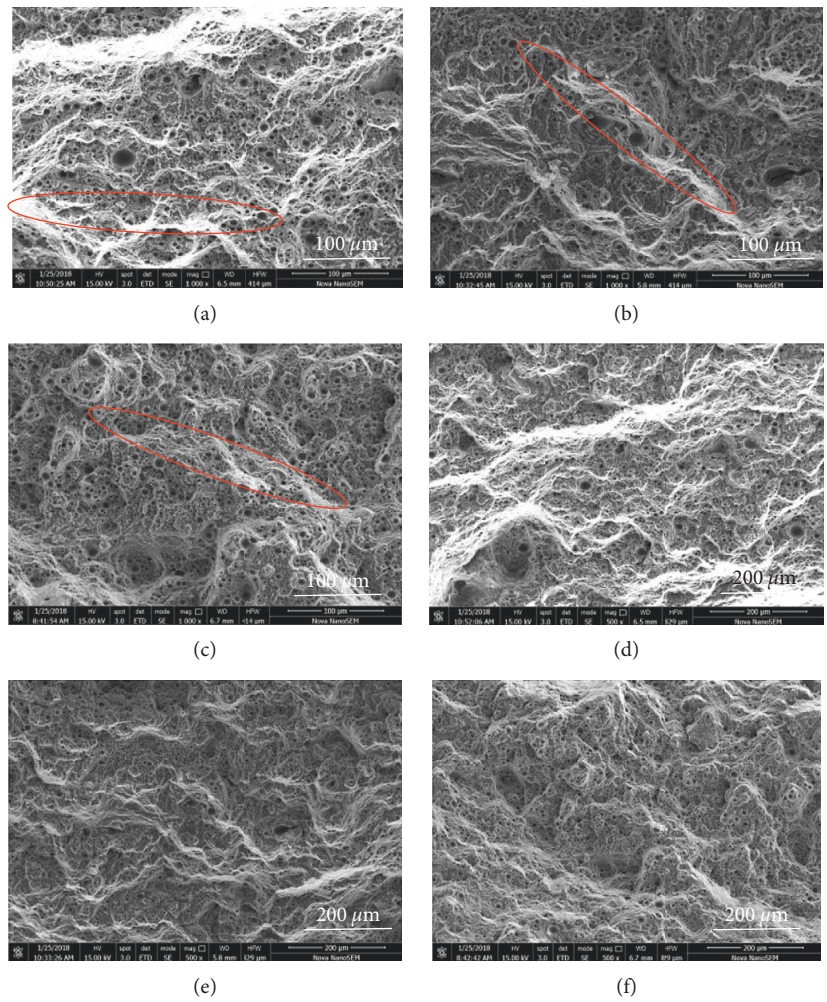

Figure 12: The typical fracture images of SLM-processed AlSi10Mg samples at (a, d) chessboard scanning, preheating temperature 80°C; (b, e) chessboard scanning, preheating temperature 120°C; and (c, f) chessboard scanning, preheating temperature 160°C.

microstructures of the top surface (XY) and side surface (XZ) of the AlSi10Mg samples prepared by SLM under different preheating temperatures and laser scanning strategies. By contrasting the microstructure, there are obvious holes in the shaped parts, that is, spherical holes and irregular holes, as shown in Figures 10(b) and 11(e). Moreover, the number of holes on the top surface of the samples is more than that on the side; although the number of side holes is small, the hole area increases obviously and presents irregular shape. Gu et al. [22] found that the "balling" produced by heat accumulation is the biggest cause of the holes, in the study of titanium alloy by laser selective melting. Compared with the chessboard scanning, in the uniformity scanning, the heat conduction direction is single and the heat dissipation efficiency is reduced. The accumulation of heat easily leads to "balling" phenomenon, in the subsequent SLM process, and the external pressure will make the molten ball rupture, that is, to produce more holes [22]. If the balling gathered and then ruptures, it will form a large concave with irregular shapes (Figure 10(b)). The balling phenomenon significantly reduced the density and interrupted the building process [23]. The balling phenomenon attributed to poor wetting between the liquid material and the substrate. Through adopting the method of increasing the preheating, the temperature gradient between the molten pool and the substrate can be reduced, so the wettability of them can be improved in the SLM process. With the increase in the preheating temperature, the holes of the specimens become small and uniform, the shape of the molten pool is obviously wider in the XY surface, but the width is uneven. The molten pool is also undulating and disorderly, and there are many joints, which cannot show integrity. In the XZ surface, the molten pool is elongated and unevenly distributed at altitude.

3.3.3. The Relationship between the Residual Stress and Microstructure. In Figures 10 and 11, the red line represents the trend of the angle of inclination of the grains. In the chessboard scanning, there is a certain overlap between the molten pool and coarsening at both ends of the pool; it shows that there is a certain overlap between the laser scanning traces in the molten pool, and there is a certain delay when it jumps between the adjacent chessboard. Under

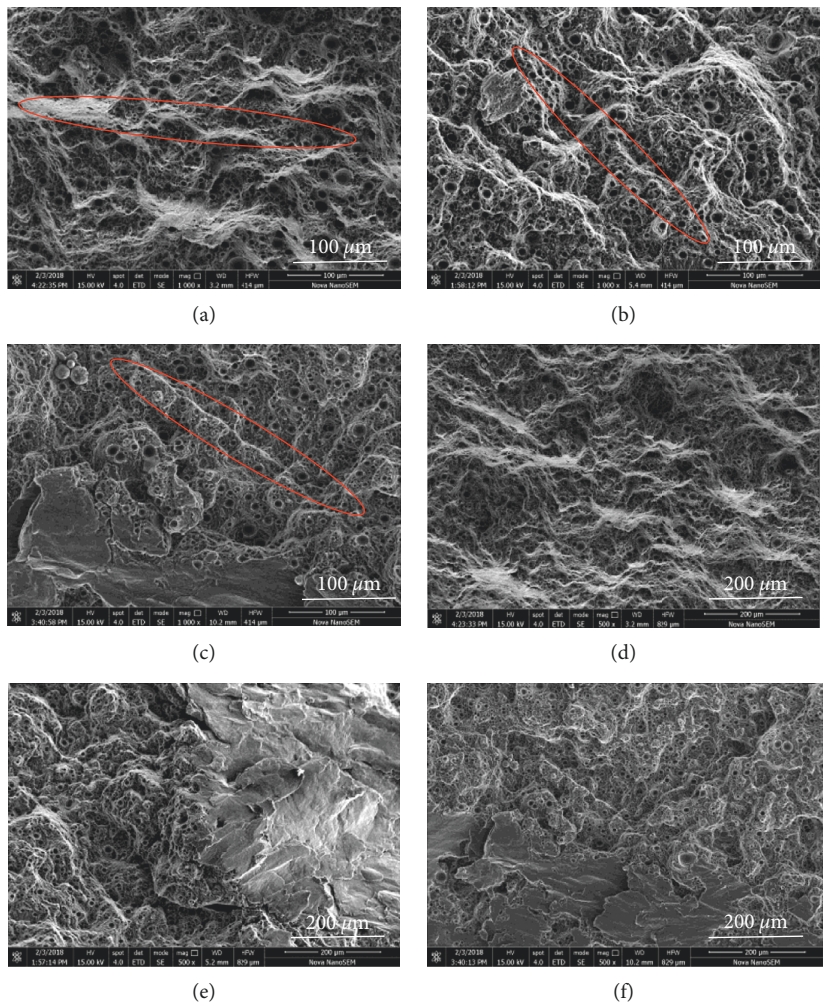

FIGURE 13: The typical fracture images of SLM-processed AlSi10Mg samples at (a, d) uniformity scanning, preheating temperature 80°C; (b, e) uniformity scanning, preheating temperature 120°C; and (c, f) uniformity scanning, preheating temperature 160°C.

the combined action of residual stresses σ_x and σ_y, the columnar grains exhibit tensile or compressive states in different directions, the grain's tilt direction is rather disordered, and there is no obvious regular relation between the grain and the residual stress.

Under the uniform scanning, the angle of scanning line between the adjacent two layers changes about 67°. In the SLM process, in order to ensure the bonding strength between layers, the laser required to penetrate the part, remelting the already processed layer. This results in the arrangement of the molten pool that has been processed, affecting the molten pool of the current layer and rendering it in a state of disorder. Compared to the chessboard scanning, the edge of the molten pool wavy is lesser than that in uniform scanning.

As shown in Figures 11(d)–11(f), under the uniformity scanning, according to the measured residual stress data (Figure 9), and preheating temperature of 160°C, the residual stress value is minimum, the residual stress value is moderate when the preheating temperature is 120°C, and the residual stress value is the highest when the preheating temperature is 80°C. And correspondingly, as the residual stress increases from small to large, in Figures 11(d)–11(f), with preheating temperature ranging from 160°C to 80°C, the angle of the columnar grain increases continuously along the clockwise direction. Preheating temperature is 80°C, the red line of the grain tilted to horizontal as is shown in Figure 11(d), compared to Figure 11(f), the residual stress causes the grain to tilt at a relatively large angle. Under the chessboard scanning, the tendency of the grain to tilt under the residual stress is the same as that of the uniformity scanning, and it shows that the microstructure of grain closely relates to residual stress in the side section surface. In the XY and XZ surfaces, the scanning strategy has little influence on the tilt angle of the grain. But, the tilt angle and morphology of the microstructure are obviously affected by the preheating temperature. It suggests that the residual stresses in different directions and sizes can effectively change the properties of the materials under the combined influence of scanning strategy and preheating temperature. It also provides effective evidence for optimizing the molding process.

In addition, fracture analysis is used to further study the effect of residual stress on the use of the product, as shown in Figures 12 and 13; under six different technological

conditions, the fracture morphology is different. The red circle in the images show the extension path of the crack. By comparison, the direction of crack path of tensile specimens are consistent with that of microstructure grain. With the increase of residual stress, both tensile fracture and microstructure showed a gradual increase of tilt angle.

It can be seen that the residual stress is directly related to the trend of microstructure and fracture morphology. The larger the residual stress value is, the greater the inclined angle of the microstructure and plastic fracture section is, which would affect the performance of the SLM products during the practical application.

4. Conclusion

In this work, the AlSi10Mg samples were fabricated by SLM using different preheating temperatures and scanning strategies. During the SLM, the AlSi10Mg parts fabricated in chessboard scanning path have higher mechanical properties or at least comparable to the parts fabricated in the uniformity scanning path. The highest elongation of the as-built AlSi10Mg parts is under the 160°C preheating conditions. The tensile strength and Vickers hardness of the as-built SLM parts preheated to 120°C are much higher than other preheating temperature conditions. Under the 80°C preheating conditions, the impact energy and density are proved to be higher than the other preheating conditions. Due to the influence of temperature gradient in the machining process, the residual stress in different parts of the specimen varies with temperature gradient. To ensure a more uniform residual stress, some measures can be taken. According to the coupling relationship between the residual stress and microstructure, the residual stresses in different directions and sizes can effectively change the properties of the materials under the combined influence of scanning strategy and preheating temperature. It also provides effective evidence for optimizing the molding process.

Conflicts of Interest

The authors declare that they have no conflicts of interest.

Acknowledgments

The authors would like to acknowledge the support of Innovation Funding of Shanghai Aerospace Science and Technology (no. SAST2016054) and Shanghai Science and Technology Talents Program Fund (no. 15QB1401400).

References

[1] K. G. Prashanth, S. Scudino, H. J. Klauss et al., "Microstructure and mechanical properties of Al-12Si produced by selective laser melting: effect of heat treatment," *Materials Science and Engineering: A*, vol. 590, pp. 153–160, 2014.

[2] T. Rajmohan, K. Palanikumar, and S. Arumugam, "Synthesis and characterization of sintered hybrid aluminium matrix composites reinforced with nanocopper oxide particles and microsilicon carbide particles," *Composites Part B: Engineering*, vol. 59, pp. 43–49, 2014.

[3] V. Umasankar, M. Anthony Xavior, and S. Karthikeyan, "Experimental evaluation of the influence of processing parameters on the mechanical properties of SiC particle reinforced AA6061 aluminium alloy matrix composite by powder processing," *Journal of Alloys and Compounds*, vol. 582, pp. 380–386, 2014.

[4] S. Ozden, R. Ekici, and F. Nair, "Investigation of impact behaviour of aluminium based SiC particle reinforced metal–matrix composites," *Composites Part A: Applied Science and Manufacturing*, vol. 38, no. 2, pp. 484–494, 2007.

[5] P. Wei, Z. Wei, Z. Chen et al., "The AlSi10Mg samples produced by selective laser melting: single track, densification, microstructure and mechanical behavior," *Applied Surface Science*, vol. 408, pp. 38–50, 2017.

[6] K. G. Prashanth, S. Scudino, R. P. Chatterjee, O. O. Salman, and J. Eckert, "Additive manufacturing: reproducibility of metallic parts," *Technologies*, vol. 5, no. 1, p. 8, 2017.

[7] D. Buchbinder, W. Meiners, N. Pirch, K. Wissenbach, and J. Schrage, "Investigation on reducing distortion by preheating during manufacture of aluminum components using selective laser melting," *Journal of Laser Applications*, vol. 26, no. 1, p. 012004, 2013.

[8] W. Huang, X. Lin, J. Chen et al., *Laser Solid Forming: Rapid Fabrication of Dense Metal Parts with High Performance*, Publishing House of Northwestern Polytechnical University, Xi'an, China, 2007, in Chinese.

[9] X. Zhou, K. Li, D. Zhang et al., "Textures formed in a CoCrMo alloy by selective laser melting," *Journal of Alloys and Compounds*, vol. 631, pp. 153–164, 2015.

[10] K. G. Prashanth, S. Scudino, T. Maity, J. Das, and J. Eckert, "Is the energy density a reliable parameter for materials synthesis by selective laser melting?," *Materials Research Letters*, vol. 5, no. 6, pp. 386–390, 2017.

[11] K. Kempen, L. Thijs, E. Yasa, M. Badrossamay, W. Verheecke, and J. P. Kruth, "Process optimization and microstructural analysis for selective laser melting of AlSi10Mg," in *Proceedings of the Solid Freeform Fabrication Symposium Conference*, pp. 484–495, Austin, TX, USA, August 2011.

[12] D. Buchbinder, H. Schleifenbaum, S. Heidrich, W. Meiners, and J. Bültmann, "High power selective laser melting (HP SLM) of aluminum parts," *Physics Procedia*, vol. 12, pp. 271–278, 2011.

[13] K. G. Prashanth, S. Scudino, and J. Eckert, "Defining the tensile properties of Al-12Si parts produced by selective laser melting," *Acta Materialia*, vol. 126, pp. 25–35, 2017.

[14] L. Salari-Sharif, S. W. Godfrey, M. Tootkaboni, and L. Valdevit, "The effect of manufacturing defects on compressive strength of ultralight hollow microlattices: a data-driven study," *Additive Manufacturing*, vol. 19, pp. 51–61, 2018.

[15] H. H. Zhu, J. Y. H. Fuh, and L. Lu, "The influence of powder apparent density on the density in direct laser-sintered metallic parts," *International Journal of Machine Tools and Manufacture*, vol. 47, no. 2, pp. 294–298, 2007.

[16] I. Shishkovsky, Y. Morozov, and I. Smurov, "Nanostructural self-organization under selective laser sintering of exothermic powder mixtures," *Applied Surface Science*, vol. 255, no. 10, pp. 5565–5568, 2009.

[17] E. Yasa, J. Deckers, and J. P. Kruth, "The investigation of the influence of laser re-melting on density, surface quality and microstructure of selective laser melting parts," *Rapid Prototyping Journal*, vol. 17, no. 5, pp. 312–327, 2017.

[18] M. Xi and S. Y. Gao, "Effect of scanning method and annealing heat treatment on microstructure and properties of laser rapid prototyping TA15 titanium alloy," *Rare Metal Materials and Engineering*, vol. 43, no. 2, pp. 445–449, 2014.

[19] J. P. Kruth, J. Deckers, E. Yasa, and R. Wauthlé, "Assessing and comparing influencing factors of residual stresses in selective laser melting using a novel analysis method," *Proceedings of the Institution of Mechanical Engineers, Part B: Journal of Engineering Manufacture*, vol. 226, no. 6, pp. 980–991, 2012.

[20] P. Mercelis and J. P. Kruth, "Residual stresses in selective laser sintering and selective laser melting," *Rapid Prototyping Journal*, vol. 12, no. 5, pp. 254–265, 2006.

[21] A. V. Gusarov, M. Pavlov, and I. Smurov, "Residual stresses at laser surface remelting and additive manufacturing," *Physics Procedia*, vol. 12, pp. 248–254, 2011.

[22] D. Gu, H. Wang, D. Dai et al., "Densification behavior, microstructure evolution, and wear property of TiC nanoparticle reinforced AlSi10Mg bulk-form nanocomposites prepared by selective laser melting," *Journal of Laser Applications*, vol. 27, no. 1, p. S17003, 2015.

[23] D. Gu and Y. Shen, "Balling phenomena in direct laser sintering of stainless steel powder: metallurgical mechanisms and control methods," *Materials and Design*, vol. 30, no. 8, pp. 2903–2910, 2009.